Preparation and characterization of germanium oxysulfide glassy films for optics

Clément Maurel, Thierry Cardinal, Philippe Vinatier, Laëtitia Petit, Kathleen Richardson, N. Carlie, François Guillen, Michel Lahaye, Michel Couzi, Frédéric Adamietz, et al.

PREPARATION AND CHARACTERIZATION OF GERMANIUM OXYSULFIDE GLASSY FILMS FOR OPTICS

C. Maurel[1,2], T. Cardinal[1], P. Vinatier[1] L. Petit[2], K. Richardson[2], N. Carlie[2], F. Guillen[1], M. Lahaye[1], M. Couzi[3] , F. Adamietz[3], V. Rodriguez[3], F. Lagugné-Labarthet[3], V. Nazabal[4], A. Royon[5], L. Canioni[5]

1- Institut de Chimie de la Matière Condensée de Bordeaux, CNRS-Université Bordeaux 1, 87 Av. Dr. Schweitzer, 33608 Pessac, France.

2- School of Materials Science and Engineering, Clemson University, 161 Sirrine Hall, Box 340971, Clemson, SC 29634, USA

3- Institut des Sciences Moléculaires, UMR 5255 CNRS, Université Bordeaux 1, 351 Cours de la Libération, 33405 Talence, France

4- Sciences Chimiques de Rennes, UMR-CNRS 6226, Equipe Verres & Céramiques, Université de Rennes 1, Campus de Beaulieu, 35042 Rennes cedex, France

5- Centre de Physique Moléculaire Optique et Hertzienne (CPMOH), CNRS-UMR 5798, 351 cours de la Libération, 33405 Talence Cedex, France.

Abstract

Homogeneous amorphous films in the GeS_2-GeO_2 system have been deposited by a RF sputtering technique. Optical characterizations has shown that the cut-off wavelength and the linear indices increase with an increase in the S/O ratio. Raman spectroscopy indicates the presence of new modes that can be assigned to intermediate germanium oxysulfide structural units. Photo-sensitivity of the oxysulfide films has been demonstrated for irradiation near the band-gap. Diffraction gratings inscribed using 488 nm exposure displayed a limited diffraction efficiency (≤3%) that weakens with a corresponding decrease in the glass S/O ratio.

Keywords

Glasses, Film, Photo-sensitivity, Oxysulfide, Raman spectroscopy

Introduction

The nonlinear optical properties of oxide and sulfide glasses have been widely studied for use in the near infrared (NIR) optical domain. Oxide glasses exhibit lower optical breakdown threshold as compared to sulfides when used in the near IR, but their nonlinear properties such as the Kerr effect, are one order of magnitude lower than that of sulfide glasses [1]. Over the last fifteen years, different results have been obtained which have examined the structuring of oxide and chalcogenide glasses materials. Sulfide glasses exhibit higher polarisability and hyperpolarisability resulting in large photosensitivity with exposure to irradiation in the visible or the NIR. Often a trade-off has to be achieved when considering the possible use of sulfides in optical devices between the photo-sensitivity, of interest for structuring based on of the linear index of the materials, and the low damage threshold at high optical power density. Oxysulfide materials which combine moderate photosensitivity and enhanced damage threshold exhibit promise in meeting such device requirements. Prior efforts in these glasses has been mainly focused on using lithium ions as dopants for conductive materials in order to improve the chemical stability of the materials without dramatically affecting the performance as electrolyte [2] [3]. So far, very little optical characterization have been performed in vitreous oxysulfides as compared to inorganic crystalline materials such as RE_2O_2S (RE : rare earth) for instance [4]. In glassy state, studies have been mainly conducted on Ga_2S_3-La_2S_3-La_2O_3 system and glasses containing germanium sulfide [5]. In term of linear and nonlinear optical indices, a compromise between the pure oxide and sulfide compositions has been found [1] [6]. The increase of the emission cross section of rare earth ions has been also recently demonstrated in TeO_2 based oxysulfide [7].

Several studies were devoted to germanium based glasses for optical applications. Photo-induced effects have been observed in GeS_2, leading, in presence of air or oxygen, to diffusion of oxygen within the glass associated with interaction with the sulfide glassy

network and to strain formation [8] [9]. Recently, the fabrication of bulk oxysulfide germanium glasses has been reported [10]. In the present work we report the synthesis of germanium oxysulfide thin film compositions in the GeS_2-GeO_2 glass system. The optical characteristics of the films for the different compositions are discussed together with their respective structural properties studied using Raman spectroscopy. Photo-induced phenomena, dependent on the sulfur to oxygen ratio, are also demonstrated for the first time.

Experimental

Targets of 5 cm diameter and of average 6 mm thickness were prepared using an appropriate mixing of GeS_2 and GeO_2 powder in order to obtain the desire S/O ratio. GeO_2 amorphous powder (Aldrich, 99.99%) with grain size centered around 10 μm were chosen for this purpose. GeS_2 was obtained by doing two thermal treatments of the same GeO_2 amorphous powder for 15 hours above the glass transition temperature at 550°C under flowing H_2S (Air Liquide Alphagaz, 99.5%) and milling the sulfinated powder between each treatment. The results of the O for S substitution were checked by weight gain, X-ray microprobe as well as by X-ray diffraction as the resulting GeS_2 materials were partially crystallized. The powder was pressed in a pellet press at a load of 5 Ton at room temperature, then the mold was heated at 120 °C prior removal of the target.

Radio-frequency (RF) magnetron sputtering of thin films was carried out in a chamber under Argon atmosphere. Pressure was maintained constant at 10^{-2} mbar throughout the whole deposition experiment. The substrate was located about 6 cm away from the target, and a 15 W plasma was created. This plasma was switched on 20 minutes prior to the deposition of the thin films to ensure removal of target surface inhomogeneity and to warrant equilibrium of the constitutive elements considering their specific pulverization rate. Under these conditions, the

deposition rate was found to vary between 3.6 Å.s^{-1} for the pure germanium sulfide target to 0.8 Å.s^{-1} for the pure germanium oxide target. The films were deposited on 1 mm thick silica substrate (fused quartz, Thuet B, spectrosil) in order to perform transmission spectra. Prior to deposition, the substrates were cleaned using ultrasonic bath and pure ethanol. Measurements with a mechanical profilometer have been used to measure the film thickness after creation of a step by masking part of the substrate during the deposition.

Auger depth profiles were mesured with a VG Microlab 310 F system. A primary electron source of 10 kV, 5 nA current was used on a 5 μm square surface. Dynamic etching of the thin films was performed with a 4 kV Ar^+ ion beam onto a 1 mm square surface with a mesured 0.5 μA current absorbed by the sample. This allowed sample to be analyzed with an accuracy of 5 atomic % for each element's profile. The position of the analyzed peaks were as follow: Ge LM2 at 1144 eV, S LM1 at 152 eV, O KL1 at 506 eV and Al KL1 at 1393 eV.

Optical transmission spectra were collected using a Varian Cary 5E spectrophotometer.

Spontaneous Raman scattering measurements were conducted using a Raman microscope (Labram, Jobin Yvon Horiba) set-up. The 514 nm lines of a mixed Krypton Argon gas laser were used as the excitation source. The incoming vertically polarized (V) laser light was focused at the front surface of the sample through a 100X microscope objective, and the polarized (V) Raman scattered light was collected using a backscattering geometry. The CCD used for collection was from ANDOR, model FI UV. The typical instrumental spectral resolution was about 6 cm^{-1}. The Rayleigh line was suppressed with a holographic notch filter. For Raman measurement, the laser irradiance was kept below 1 kW/cm^2 in order to avoid any photo-induced effects. For irradiance of 100 kW/cm^2, it was determined that such photo-induced effect could be distinguished on sulfide and oxysulfide films after 15 and 30 seconds of exposure. These times were identified as the threshold for modification and were used in subsequent exposure experiment.

Thickness and linear refractive indices at 1064 nm and 532 nm were obtained using an extended Brewster angle reflection method over the ± [10°; 80°] wide θ range. Best fits to the experimental patterns were conducted using a unique optical layer model, for both reflected R_{pp} signals collected at 1064 nm and 532 nm; these measurements include an original multi-reflection layers procedure developed previously by our group [11]. This original procedure allows one to minimize errors on thickness, indices and also includes determination of the optical dispersion. The accuracy of the obtained indices of refraction from this ellipsometry measurement was better than 0.01.

The 488 nm wavelength of an Argon Laser has been used for recording the volume gratings on the films. The p-polarized Argon beam was first split using a 50/50 cube beamsplitter and recombined at the sample in order to obtain interferences fringes (figure 1). The angle between the two beams was about 2θ=30° leading to a periodicity of about 1 μm step according to Bragg's law. The diffraction efficiency of the photo-induced volume gratings was precisely measured by recording the intensity of the first diffracted order from a HeNe Laser at 632.8 nm perpendicular to the surface of the film which was used as the probe beam. The total irradiance of the actinic 488 nm light was set to about 300 $mW.cm^{-2}$. All sulfide and oxysulfide films were exposed during 30 minutes, at which point no clear variation in intensity of the first order of diffraction of the probe beam could be seen anymore.

Results

Auger spectroscopy was used to study the chemical composition of the films as a function of film depth. These measurements were performed on films nominally 1 μm thick which had been deposited on aluminum foil substrates. This spectroscopy, coupled with ion etching, has allowed us to evaluate the film composition throughout its thickness to examine evidence of compositional variation during film deposition. For oxysulfide thin films, it was determined

that the S/O ratio was found to be constant through the thickness of the sample. The result presented on figure 2 for GeOS thin film clearly indicates a homogeneous composition of the film throughout its depth. The etching rate of the film samples were found to vary slightly depending of the film's Oxygen / Sulfur ratio. Etch rates ranged from 1.5 $Å.s^{-1}$ for pure GeO_2 film to 2.0 $Å.s^{-1}$ for pure GeS_2. The compositions were in agreement with the compositions of the targets. These composition measurements were cross-checked and reconfirmed by X-Ray microprobe.

Transmission spectra were collected from 1000 nm to 200 nm. The oscillations observed (not shown here) in the range between 1000 nm and the strong absorption in the visible UV frontier corresponds to the interference due to the index contrast between the film and the silica substrate. Absorption spectra were extracted in the UV range assuming that for high absorption coefficient of the film deposited interferences vanish due to disappearance of contrast. The absorption spectra of the films have been corrected or Fresnel reflections. They are reported in figure 3, plotted in logarithm scale of the absorption coefficient versus wavelength. In the UV region a progressive decrease of the wavelength position of the band edge as the oxygen content increase can be seen from about 430 nm for GeS_2 to about 270 nm for GeO_2.

Ellipsometry measurements have been conducted on GeS_2, GeOS and GeO_2 thin films deposited on silica substrates. Figure 4 exhibits the results of the GeOS and GeS_2 films. The ellipsometric treatments have shown that all films can be described as two-layers systems, including a thick bottom bulk layer corresponding to the expected composition and a second thin layer at the top of the film, but with lower index of refraction. For the germanium sulfide sample, the top layer has been evaluated as nominally 20 nm thick. For germanium oxysulfide and germanium oxide samples, thicker top layers of ~100 nm have been estimated. The obtained optical parameters, i.e. linear index values n_0 and thicknesses d, are gathered in table

1. The full thicknesses including both layers of the film are in agreement with the measurements done by the mechanical profilometer. For GeS_2 and GeO_2 films, the linear index values of bottom layers (the thickest one) are in full agreement with those expected for the corresponding bulk materials [12] [13]. In addition, both linear index of the thin top and bottom layers decrease with the oxygen concentration rise until they reach some minima for GeO_2 film. The value of the linear susceptibility $\chi^{(1)}$ ($n_0^2 = 1 + \chi^{(1)}$) of the oxysulfide composition corresponds to the average of the sulfide and oxide pure composition values taking into account the accuracy of the measurement (±0.01).

For comparison purpose, all Raman spectra of the five studied composition (GeO_2, $GeO_{1.4}S_{0.6}$, GeOS, $GeO_{0.6}S_{1.4}$, GeS_2) were normalized to the most intense band because of the different Raman scattering cross-sections between sulfide and oxide samples. Therefore, sulfur-rich glasses exhibited a Raman signal at least one order of magnitude larger than oxygen-rich compositions due to the difference of polarisability between oxide and sulfide compounds. They are presented in Figure 5. In the spectrum range between 200 cm^{-1} and 325 cm^{-1}, for compositions from GeS_2 to GeOS, two bands located at 235 cm^{-1} and at 255 cm^{-1} can be distinguished. The later band increases in relative intensity with the progressive increase of the oxygen concentration. Similar bands at 250-260 cm^{-1} have been reported by several authors as the ethane-like $S_3Ge\text{-}GeS_3$ units in which Ge atoms occupy corner site in GeS_4 tetrahedra in rich germanium samples [14] [15]. Recently, it had also been proposed that such vibration could appear also for three-fold coordinated sulfur atoms [16]. For larger oxygen concentration than that of the GeOS composition, no clear vibrational mode can be distinguished, but only a broad signal that could correspond to vibrational contributions involving sulfur and oxygen atoms. For the GeO_2 film composition, a band is observed at 345 cm^{-1}.

In the spectral range between 315 cm^{-1} and 650 cm^{-1}, the maximum of the broad Raman signal is progressively shifted from 342 cm^{-1} to 423 cm^{-1} as the oxygen concentration increases. These Raman spectra were simulated using Gaussian function and so, the spectrum for GeS_2 could be simulated using 5 main vibrations located at 345 cm^{-1}, 375 cm^{-1}, 410 cm^{-1}, 430 $cm^{-1}$and 480 cm^{-1} (figure 6a). The main band around 342 cm^{-1} has been associated to A_1 symmetric stretching vibrations of S atoms in GeS_4 units, and the vibration around 375 cm^{-1}, usually called the companion A_1^C band, is attributed to edge sharing tetrahedral sites [17]. For the weakest band at 410 cm^{-1}, the situation is not clear. According to Jackson et al., a band located around 400 cm^{-1} could come from edge sharing GeS_4 units. The bands around 430 cm^{-1} and 475 cm^{-1} have been attributed respectively to short S-S chains between GeS_4 units and S-S bond stretching vibrations in S_8 like rings [14-15][18][19].

The fitted Raman spectrum of GeO_2 film is reported in figure 6b. Five Gaussian bands at 340 cm^{-1}, 425 cm^{-1}, 480 cm^{-1}, 550 cm^{-1} and 590 cm^{-1} are necessary to fit this spectrum. In the literature a band at 347 cm^{-1} has been assigned to germanium motions in deformation modes of the glass network. The main band around 420 cm^{-1} has been attributed to symmetric stretching mode of Ge-O-Ge bridging oxygen atoms between GeO_4 tetrahedral sites. The vibration at 520 cm^{-1} has been assigned to the breathing motion of oxygen atoms in 3-membered GeO_4 rings. Vibrations between 500 cm^{-1} to 620 cm^{-1} were associated to bending modes of Ge-O-Ge bridges. [20].

In a first approach, summations of the bands obtained from the simulation of pure GeO_2 and GeS_2 were used for to fit the spectral profiles of oxysulfide glasses. For the three compositions studied, the addition of a new band between 360 cm^{-1} and 400 cm^{-1} is necessary to correctly simulate these spectra. This band becomes the prominent one for the composition $GeO_{1.4}S_{0.6}$.

Photo-induced modifications of the films were obtained for sulfide and oxysulfide compositions. Figure 7 illustrates the Raman spectra of GeOS composition after 15 and 30 seconds of exposure with about 100 kW/cm^2 irradiance. After irradiation, between 360 cm^{-1} and 420 cm^{-1} a very similar shoulder to those already observed can be distinguished in the same spectral range with all sulfide and oxysulfide compositions. Exposure with a larger laser power density leads to an increase of the intensity of this band but also to damage of the surface of the glass, visible with an optical microscope.

Interference patterns have been written using Argon laser emitting at 488 nm with a low irradiance (300 mW/cm^2). The first order of diffraction intensity at 632.8 nm was measured following 30 minutes of exposure for sulfide and oxysulfide films (table 2). The diffraction intensities increase when the sulfur to oxygen ratio increases. First order diffraction efficiencies decrease from 3% for GeS_2 to ≤0.3% for $GeO_{1.4}S_{0.6.}$ It has been checked that the gratings remain unchanged after one week.

Discussion

Homogeneous oxysulfide thin films were obtained, with adjustable compositions correlated to the composition of the target used for RF sputtering. The absorption band edge of the films prepared in the system Ge-O-S are directly dependent on their sulfur content and systematically red shift with an increase in the S/O ratio (figure 3). As the sulfur concentration increases, the wavelength position of the band edge increases as suggested by ellipsometry measurements which exhibit a concurrent increase of the linear index with an increase in sulfur content. This effect is directly related to the larger polarisability of the sulfur ions as compared to the oxygen ions, which is followed by a lower band gap of the material. The GeOS composition exhibits a linear susceptibility which is the average between GeO_2 and GeS_2 film values suggesting that the evolution seems to be linearly dependant on

the S/O ratio. This feature indicates that in terms of the refractive index evolution, sulfur replaces for the oxygen in the glass network without significant modification of the glass structure. The near-surface layers of the oxysulfide and oxide films exhibit a lower index of refraction. According to Auger spectroscopy, surface oxidation does not appear to be primarily responsible as the individual glass constituent distribution within the composition was found to be homogeneous in the depth of the sample. Nevertheless, we can not exclude a surface contamination by oxygen of about 10-20 nm which is below the detection limit in the Auger profile. A proposed hypothesis for this observation may involve some form of surface hydrolysis in the film that leads to a decrease of the density of the film without a strong diffusion of oxygen. Further investigations examining post deposition annealing may provide further insight into these observations, as no annealing was performed on the fresh films examined in this study.

The Raman spectroscopy indicates a progressive evolution of the glass structure from GeS_2 up to GeO_2 as the S/O ratio decreases. The vibrational features of GeO_2 and GeS_2 have been the subject of multiple articles [14][20]. The main bands located at 430 cm^{-1} and at 342 cm^{-1} correspond respectively to GeO_4 and GeS_4 vibrations. As the oxygen concentration increases, a shoulder can be distinguished at the high wavenumber side of the GeS_2 main vibration. For larger oxygen concentrations corresponding to the glass composition $GeO_{1.4}O_{0.6}$, this shoulder gives rise to a new band in between 360 cm^{-1} and 430 cm^{-1}, confirming the signature of new vibrational species different from GeO_4 or GeS_4 tetrahedral sites. Such a vibration could be related to the formation of entities such as GeO_3S, GeO_2S_2 or $GeOS_3$ tetrahedral units consistent with the suggestion of Kim et al's analysis of bulk oxysulfide glasses that germanium atoms are coordinated with both sulfur and oxygen [10]. Concerning the vibrations located at 235 cm^{-1} and at 255 cm^{-1} the interpretation is less clear. Such vibrations, usually assigned to the ethane-like $S_3Ge\text{-}GeS_3$ entities, tend to appear for sulfur-deficient

samples. In our case, we can not exclude the possibility that such phenomenon occur during film deposition. The chemical analysis using X Ray microprobe and Auger spectroscopy for sulfur and in particular for oxygen did not allow accuracy better than 5%. For the compositions with large oxygen concentration $GeO_{1.4}S_{0.6}$ and GeO_2, these bands cannot be observed, suggesting the disappearance of $S_3Ge\text{-}GeS_3$ bridges. No additional band could be observed that could be related to the formation of similar homopolar bridges in oxysulfide environment.

Irradiation of the film at 514 nm induced, for large irradiance, structural changes on sulfur-rich germanium oxysulfide and GeS_2 films (fig 7). The shoulder appearing in the Raman spectra between 360 cm^{-1} and 420 cm^{-1} has to be related to the new band observed for oxysulfide compositions. This band is attributed to the mixed sulfur and oxygen tetrahedral environment of the germanium ions. Such an effect could provide evidence of oxygen diffusion most probably from the top of the film or phase separation of the glass structure in the case of oxysulfide films. Considering the difference in the Raman cross-section of the sulfide and oxysulfide vibrations, these datas suggest significant species vibrating around 385 cm^{-1} have been formed upon illumination. Tanaka et al. suggested for GeS_2 that following light exposure in air Ge-Ge bridges break leading to formation of Ge-O-Ge bonds and photobleaching [21]. However in similar material, such as $GeSe_2$, light illumination could be coupled, as Spence et al. mentioned [9], to strain appearance in the network leading to photodarkening. In the case of oxysulfide and sulfide films, the feature around 250 cm^{-1} in the Raman spectra could indicate that the Ge-Ge bridges are present for GeOS, $GeO_{0.4}S_{1.6}$ and GeS_2, however in this study no specific evolution could be observed (figure 5).

Interference patterns created upon exposure of the films at lower irradiance at 488 nm near the band gap has allowed recording Bragg gratings. The first order diffraction efficiency at 632.8 nm was found to increase with an increase in the sulfur to oxygen ratio, in agreement with a

lower band gap for sulfur-rich film materials content which exhibit and an increase in absorption coefficient at 488 nm (figure 3). The diffraction efficiency measurement clearly demonstrates the presence of a volume grating. Spatially resolved Raman measurements using micro Raman apparatus could not clearly denote a modification in the Raman spectral features even though patterning can be seen using optical microscope and remains stable after several weeks. It is believed that grating inscription with shorter wavelengths and/or higher irradiances should be used to realize gratings with higher diffraction efficiencies.

Conclusion

Oxysulfide thin films have been obtained in the GeS_2-GeO_2 glass system using magnetron RF sputtering of mixed oxide and sulfide targets. Optical and vibrational spectroscopic measurements indicate a progressive evolution of the properties from the oxide to the sulfide as the sulfur concentration increases. A new band located around 385 cm^{-1} attributed to a mixed anion (sulfur and oxygen) germanium tetrahedral sites has been observed by Raman spectroscopy. First photo-induced gratings have been observed in these new optical materials upon exposure with UV irradiation.

Acknowledgments

This work was carried out with the support of a number of research, equipment, and educational French and US grants, including the Agence Nationale de la recherche ANR (grant ANR-05-BLAN-0212-01), the CNRS PICS grant 3179, a FACE grant from the French Embassy in the US, and funding from the National Science Foundation (international REU grant EEC-0244109) and DMR-031208.

Table Captions

Table 1

Variation in refractive indices as a function of thin film compositions and thickness, for near and sub-surfaces regions of the glass films, obtained from ellipsometry measurements

Table 2

First order diffraction efficiency of sulfide and oxusulfide thin films compositions measured at 632.8 nm.

Composition	Sulfur percent (%)	Thickness (d) / Refractive index (n_0)					
		Film			Top layer		
		d_1 (nm) ± 5 %	n_0 ± 0.01 (532 nm)	n_0 ± 0.01 (1064 nm)	d_2 (nm) ± 5 %	n_0 ± 0.01 (532 nm)	n_0 ± 0.01 (1064 nm)
GeO_2	0	1093	1.77	1.69	98	1.68	1.65
GeOS	50	2670	1.89	1.85	119	1.75	1.71
GeS_2	100	8330	2.11	2.06	19	1.80	1.75

Table 1

Composition	First order Diffraction efficiency (%) at 632.8 nm
GeS_2	2.82
$GeO_{0.4}S_{1.6}$	2.45
GeOS	1.30
$GeO_{1.4}S_{0.6}$	0.27

Table 2

Figure captions

Fig 1

Experimental set up for grating inscriptions in sufide and oxysulfide thin films

Fig 2

Auger spectroscopic depth profile illustrating chemical composition of resulting GeOS thin films deposited on aluminum substrate

Fig 3

Absorption spectra of oxysulfide thin films

Fig 4

Ellipsometry measurements on GeOS (a) and GeS_2 (b) thin films at 532 nm.

Fig 5

Raman spectra of the investigated films. λ_{exc} = 514 nm

Fig 6

Fitting of Raman spectra of GeS_2 (a) and GeO_2 (b) thin films using Gaussian functions.

Fig 7

Raman spectra of GeOS film measured before and after irradiation. Irradiation has been conducted at 514 nm with an irradiance of 100kW/cm^2

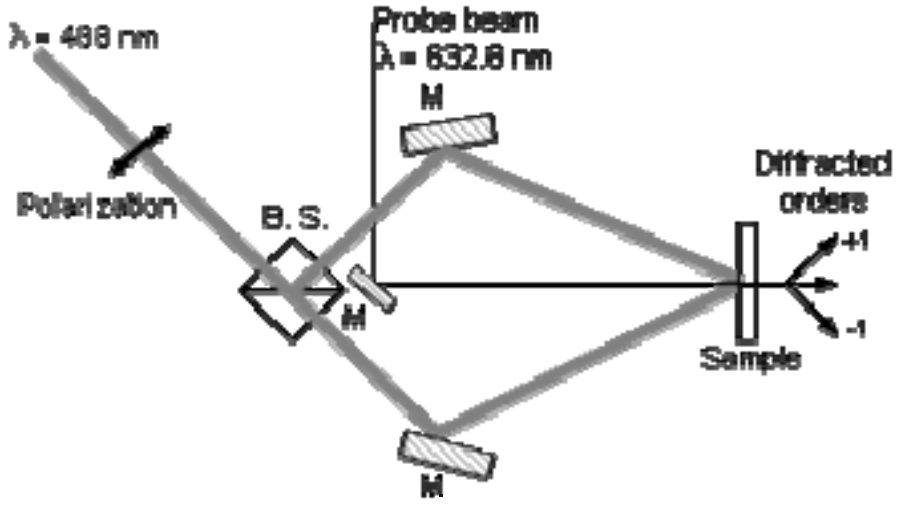
λ = 488 nm
Probe beam
λ = 632.8 nm
M
Polarization
B. S.
M
Diffracted
orders
+1
-1
Sample
M

Fig 1

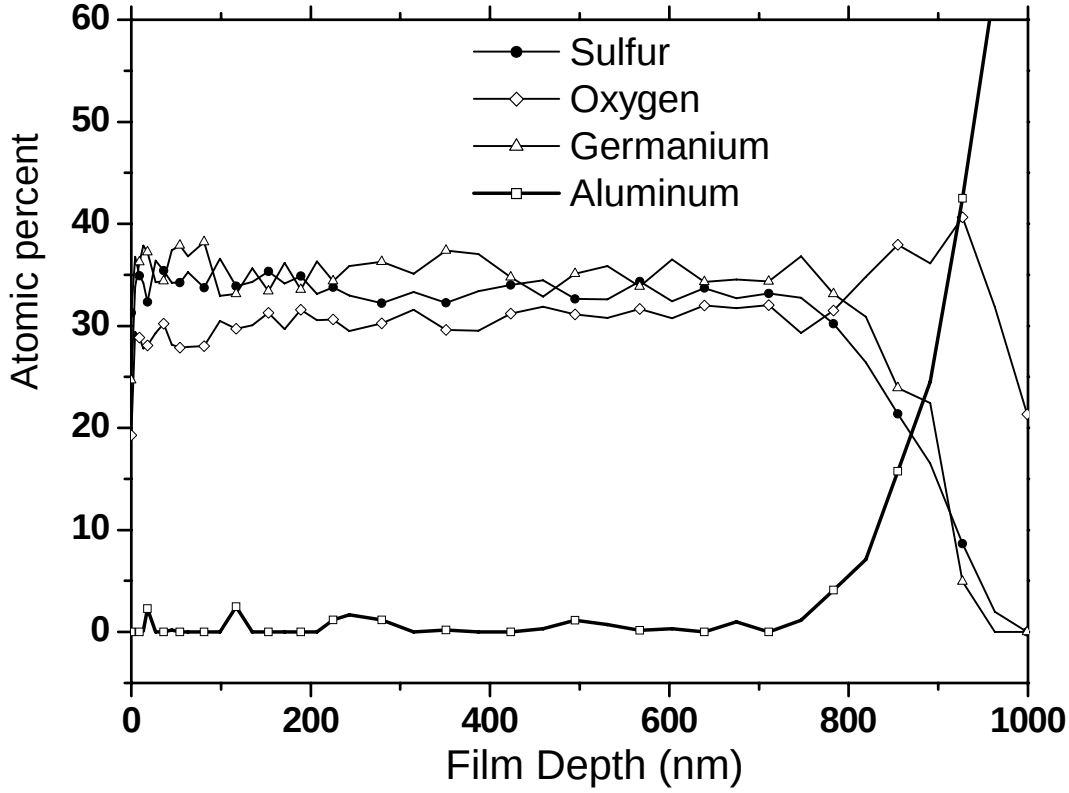
Sulfur
Oxygen
Germanium
Aluminum
Atomic percent
Film Depth (nm)
0
10
20
30
40
50
60
0
200
400
600
800
1000

Fig 2

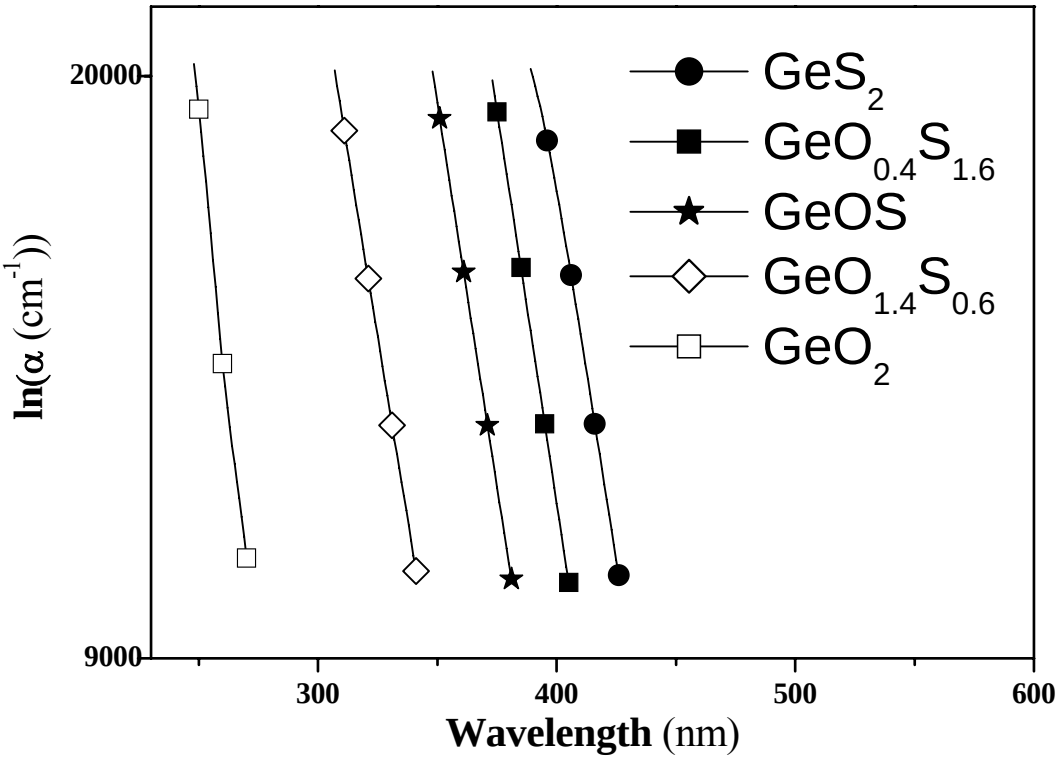
20000
9000
300
400
500
600
ln(α (cm-1))
Wavelength (nm)
GeS2
GeO0.4S1.6
GeOS
GeO1.4S0.6
GeO2

Fig 3 :

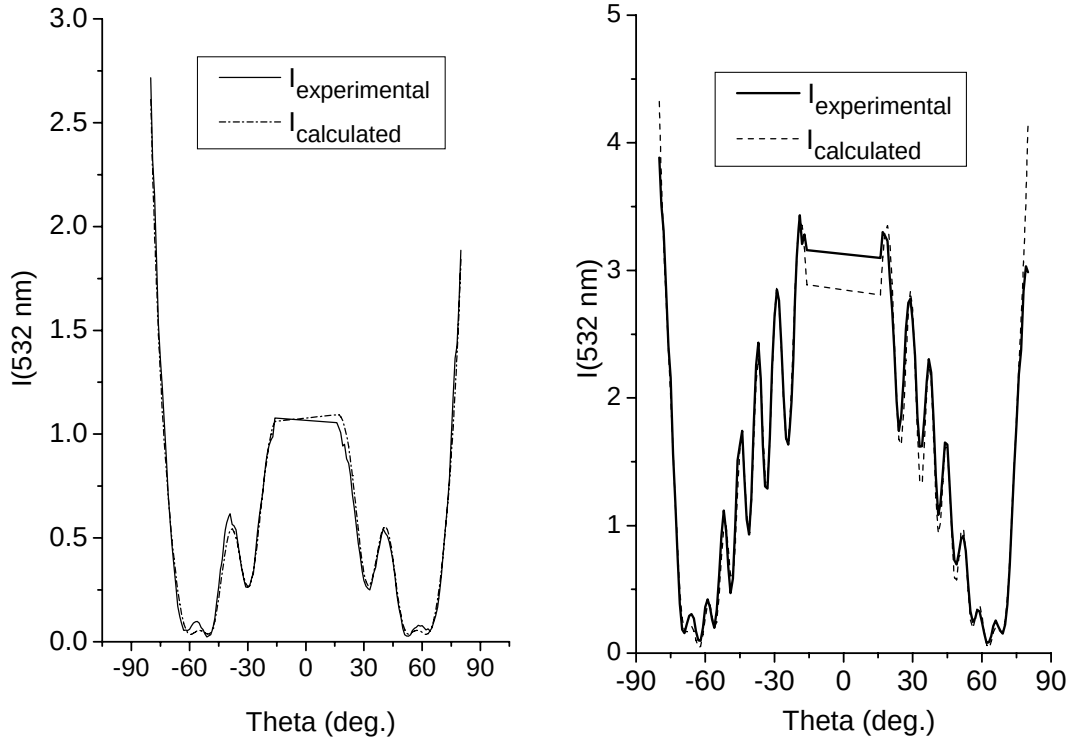

(a) GeOS (b) GeS_2

Fig 4

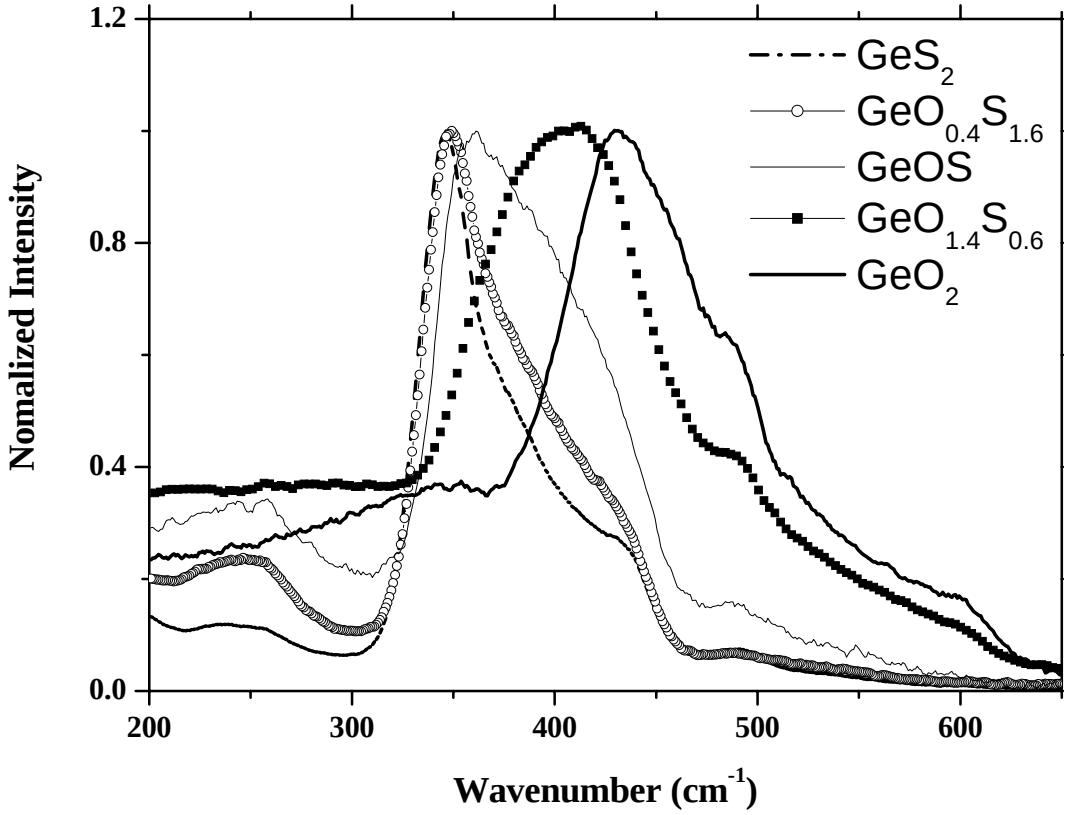
1.2
0.8
0.4
0.0
200
300
400
500
600
Nomalized Intensity
Wavenumber (cm-1)
GeS2
GeO0.4S1.6
GeOS
GeO1.4S0.6
GeO2

Fig 5

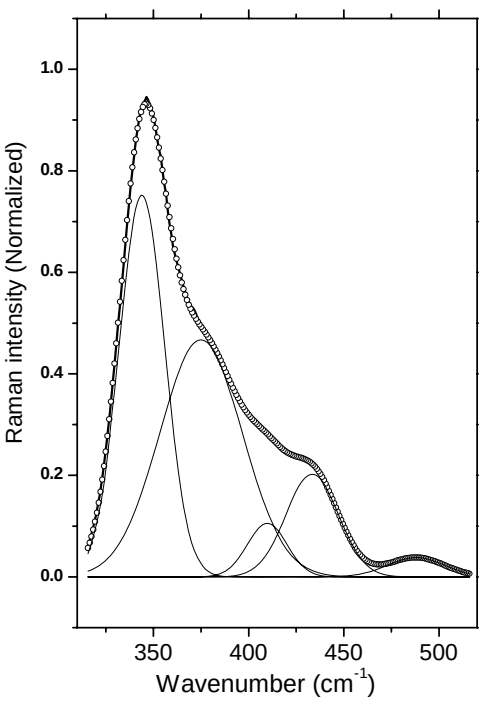
Raman intensity (Normalized)
1.0
0.8
0.6
0.4
0.2
0.0
350
400
450
500
Wavenumber (cm-1)

(a)

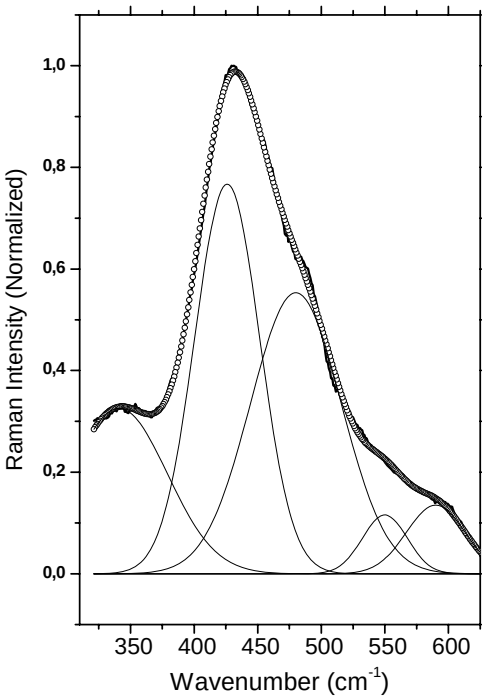
Raman Intensity (Normalized)
1,0
0,8
0,6
0,4
0,2
0,0
350
400
450
500
550
600
Wavenumber (cm-1)

(b)

Fig 6

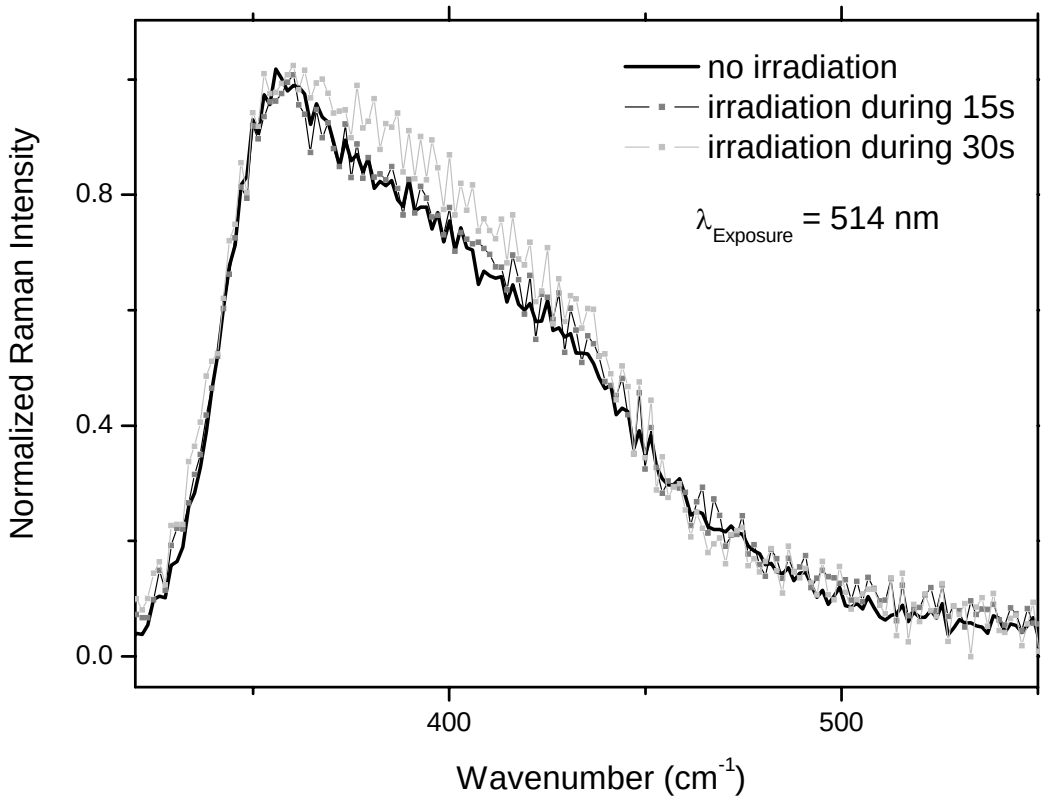
no irradiation
irradiation during 15s
irradiation during 30s
λExposure = 514 nm
Normalized Raman Intensity
0.0
0.4
0.8
400
500
Wavenumber (cm-1)

Fig 7

[1] Z. H. Zhou, H. Nasu, T. Hashimoto, K. Kamiya, Jour. Mater. Res. 14-2 (1999), 330.

[2] K. H. Joo, P. Vinatier, B. Pecquenard, A. Levasseur, H. J. Sohn, Solid State Ionics, Diffusion and Reactions 160 (2003), 51.

[3] M. Tatsumisago, K. Hirai, T. Hirata, Solid State Ionics 86-88 (1996), 487.

[4] T. Nishimura, K. Nomoto, K. Yokota and M. Tamatani, Mat. Res. Bull. 10 (1975), 747.

[5] M. Guittard, A. M. Loireau Lozac'H, F. Gerguer, S. Barnier, J. Flahaut., J. Solid State Chem. 62 (1986), 191.

[6] H. Yayama, S. Fujino, K. Morinaga, H. Takebe, D. W. Hewak, D. N. Payne, J. Non-Cryst. Solids 239 (1998), 187.

[7] G. Wang, S. Xu, S. Dai, J. Zhang, L. Hu, Z. Jiang, Mater. Lett. 59 (2005), 366.

[8] T. Kawaguchi, S. Maruno and K. Tanaka, J. Appl. Phys. 73 (1993), 4560.

[9] C. A. Spence, S. R. Elliott, Physical Review B 39-8 (1989), 5452.

[10] Y. Kim, J. Saienga and S. W. Martin, J. Non Cryst Solids 351 (2005), 1973.

[11] V. Rodriguez and C. Sourisseau, J. Opt. Soc. Am. B 19 (2002), 2650.

[12]N. Terakado, K. Tanaka, Journal of Non Cryst. Solids 351 (2005), 54.

[13] C. C. Huang, D. W. Hewak, Optics Express 12 (2004), 2501.

[14] I. P. Kotsalas, C. Raptis, Phys. Rev. B 64 (2001), 125210.

[15] K. Jackson, A. Briley, S. Grossman, D. V. Porezag, M. R. Pderson, Phys. Rev. B 60 (1999), 14985.

[16] S. Blaineau, P. Jund, Phys. Rev. B 69 (2004), 06201.

[17] S. Sugai, Phys. Rev. B 35 (1987), 1345.

[18] G. Lucovsky, F. L. Galeener, R. C. Keezer, R. H. Geils, H. A. Six, Phys. Rev. B 10 (1974), 5134.

[19] A. T. Ward, J. Phys. Chem. Vol 72 (1968), 4133.

[20] M. Micoulaut, L. Cormier, G. S. Henderson, J. Phys. Condens. Matter 18 (2006), 753.

[21] K. Tanaka, Y. Kasanuki, A. Odajima, Thin Solid Films 117 (1984), 251.